Available online at www.ijpsdr.com

International Journal of Pharmaceutical Sciences and Drug Research 2018; 10(6): 460-473

Research Article

ISSN: 0975-248X
CODEN (USA): IJPSPP

Hetero-Binuclear Complexes of Lanthanum (III) Using Bridging *N,N'*-Bis(2-Pyridylmethyl)Oxamide and Terminal 1,10-Phenanthroline: Synthesis, Characterization and Biological Evaluation

P. R. Chetana[1*], Vibha Vinayakumar Bhat[1], Mohan A. Dhale[2]

[1]*Department of Chemistry, Central College Campus, Bangalore University, Bengaluru – 560001, Karnataka, India*
[2]*Microbiology and Fermentation Technology Department, Central Food Technological Research Institute, Mysore – 570020, Karnataka, India*

ABSTRACT

In the present study, hetero-binuclear La(III) complexes were newly synthesized using well known bridging ligand N,N'-bis(2-pyridylmethyl)oxamide (2PMO, **1**) and "complexes as ligands" [Cu(2PMO)] (**2**) and [Ni(2PMO)] (**3**). The newly synthesized mononuclear (**4**) as well as hetero-binuclear complexes (**5** and **6**) were characterized by analytical and spectroscopic techniques. The newly synthesized complexes were tested for their binding ability towards CT-DNA and chemical nuclease property towards SC pUC 19 DNA. The complexes were tested for antibacterial activities against Gram negative bacteria (*E. coli* and *K. pneumonia*) and Gram positive bacteria (*B. subtilis* and *S. aureus*), antioxidant activities by DPPH radical scavenging and ferrous-ion chelation methods and cytotoxicity against MCF-7 cell lines by MTT assay. The structure-activity relationship revealed that the newly synthesized hetero-binuclear complexes show potent DNA binding and chemical nuclease activities, antibacterial, antioxidant and cytotoxic activities.

Keywords: Antibacterial, antioxidant, antitumor, DNA interactions, oxamides, Lanthanum (III) complexes.

DOI: 10.25004/IJPSDR.2018.100606 **Int. J. Pharm. Sci. Drug Res. 2018; 10(6): 460-473**

***Corresponding author**: Prof. P. R. Chetana
Address: Department of Chemistry, Central College Campus, Bangalore University, Dr. B. R Ambedkar Veedhi, Bengaluru – 560001, Karnataka, India
E-mail ✉: pr.chetana@gmail.com
Relevant conflicts of interest/financial disclosures: The authors declare that the research was conducted in the absence of any commercial or financial relationships that could be construed as a potential conflict of interest.
Received: 28 August, 2018; **Revised:** 03 October, 2018; **Accepted**: 16 October, 2018; **Published:** 20 November, 2018

INTRODUCTION

The cleavage of DNA by metal complexes is of considerable interest in current pharmaceutical industries. Chemical nuclease activity by metal complexes usually takes place either by hydrolytic pathway where phosphodiester bond is hydrolyzed or oxidative pathway which involves abstraction of proton from sugar-phosphate backbone or nitrogenous bases. Hydrolytic pathway results in the 3′-OH and 5′-OPO_3H fragments that can be relegated by natural enzymes whereas oxidative pathway results in the formation of non-sticky ends which cannot be relegated

by natural enzymes. [1-2] The oxidative pathway is catalyzed by the activation of metal complex in presence of oxidizing agent or reducing agent to generate diffusible free radicals which damage DNA. Thus, cleavage of DNA by oxidative pathway by metal complexes is highly beneficial in designing antitumor and antimicrobial agents. The chemical nuclease activity of the metal complexes depends on their interaction with DNA. The modes of non-covalent interactions include electrostatic effect, groove binding and intercalation of metal complexes with DNA or proteins are directed by the nature of the ligand, metal centers, geometry and coordination sphere of the metal complexes. [3-6] The efficiency of the metal complex in binding to the DNA is decided by the type of coordinated ligand. The presence of extended aromatic planar ring in the ligand moiety directs the metal complex in targeting DNA. [7] The oxidative stress induced by the free radicals that are generated in human body by various metabolic processes releases many free radicals such as hydroxyl radicals, superoxide radicals, singlet oxygen etc. The enzymes in the body to counteract these ions are limited and in turn these radicals are responsible for life threatening diseases such as carcinogenesis, inflammations etc. The compounds having the ability to suppress the activities of these free radicals are known as antioxidants. [8-9] These free radicals if produced in excess can cause oxidative damage of the DNA that causes cancerous effects. Thus, there is a need for drug molecules which possess diversified applications such as chemical nuclease activities, antimicrobial, antioxidant and antitumor activities are highly beneficial.

The coordination of suitable ligands also decides the biological properties of the metal complexes. Ligands having bioactive moieties such as –C=O, –NH, –SH, –OH and aromatic planar rings can enhance the antimicrobial properties of the metal complexes. The coordinating ligands increase the lipophilicity of the complexes by sharing the positive charge on the metal ions by chelation thereby enhancing the permeability of the complexes into biological membranes. [10] These properties introduce metal complexes as potent antimicrobial agents.

The structure and geometry of the metal complexes decide the biological role of the metal complexes. In this regard, several investigations have been carried out in exploring the pharmaceutical values of lanthanum(III) complexes. La(III) in its stable +3 oxidation state mimics biological ions such as Ca^{2+} and K^{+} and hence can be highly beneficial in synthesizing chemical nucleases. [11] La(III) complexes have been used as probes in immunoassays and as MRI agents, [12-14] anticancer agents, [15–19] binding agents towards DNA, RNA, proteins and as chemical nucleases, [20-24] antimicrobial agents [25-30] as well as antioxidant agents. [31-32] In this view, herein we report the synthesis and characterization of mononuclear as well as hetero-binuclear complexes containing lanthanum(III), copper(II) or nickel(II) ion bridged by versatile ligand N,N′-bis(2-pyridylmethyl)oxamide and ancillary ligand 1,10-phenanthroline which is a classical DNA intercalator. We aimed to evaluate their biological properties such as DNA interactions, antibacterial, antioxidant and antitumor activities by standard procedures. The newly synthesized hetero-binuclear complexes were found to possess higher DNA binding strengths towards CT-DNA, chemical nuclease activity towards SC pUC19 DNA, antibacterial activity against Gram negative bacteria (*E. coli* and *K. pneumonia*) and Gram positive bacteria (*B. subtilis* and *S. aureus*), free radical scavenging and metal ion chelating abilities and antitumor activities against MCF-7 cell lines. Thus, they can be utilized as potent diagnostic as well as pharmaceutical tools.

MATERIALS AND METHODS

Materials

All the reagents and chemicals were obtained from Sigma Aldrich (USA) and Fluka (USA) and used as obtained. Solvents used for spectroscopic and electrochemical procedures were purified by standard procedure reported earlier. [33] Super coiled (SC) pUC 19 DNA (cesium chloride purified) was purchased from Bangalore Genei (India). Calf-thymus DNA (CT-DNA), Agarose (molecular biology grade), Ethidium bromide (EB) was obtained from Sigma Aldrich (USA). 2,2-diphenyl-1-picrylhydrazyl (DPPH), Ferrozine (Extra pure) were purchased from Himedia and used as received. Ferrous chloride and Tris (tris-hydroxymethyl(aminomethane)) were purchased from Merck and used as purchased. Tris-(hydroxymethyl) aminomethane-HCl (pH = 7.2) buffer solution was prepared using deionized, double distilled water.

Bacterial media was purchased from Himedia. The bacterial strains *Escherichia coli* (ATCC 25922), *Klebsiella pneumonia* (MTCC 109), *Staphylococcus aureus* (MTCC 3160) and *Bacillus subtilis* (MTCC 441) were procured from IMTECH, Chandigarh, India. Human breast cancer cells (MCF-7) were purchased from ATCC. Foetal bovine serum (FBS), penicillin (100 IU/mL), streptomycin (100µg/mL), glutamine, RPMI-1640, 3-(4,5-dimethylthiazol-2-yl)-2,5-diphenyltetrazolium bromide (MTT), dimethyl sulfoxide (DMSO) chemicals required for cytotoxicity studies were purchased from Hi-media (Mumbai, India).

Methods

Syntheses

The ligand N,N′-bis(2-pyridylmethyl)oxamide (2PMO, **1**), [34] [Cu(2PMO)] (**2**) and [Ni(2PMO)] (**3**) were synthesized by modifying literature procedure [35] for the comparison of their activities with those of newly synthesized mononuclear and binuclear-complexes. The new mononuclear $[La(2PMO)(NO_3)_2](NO_3)$ (**4**) and hetero-binuclear complexes **5-6** were synthesized by following reported methods with modifications. [36]

Synthesis of $[La(2PMO)(NO_3)_2](NO_3)$ (4)

Diethyl oxalate (0.408 mL, 0.1 M) and 2-(aminomethyl)pyridine (0.432 mL, 0.2 M) were dissolved in 20 mL ethanol. The solution was refluxed at 60 ˚C for 1 h. Aqueous solution of $La(NO_3)_3.6H_2O$ (0.433 g, 0.1 M) was added to the above reaction mixture and refluxing was continued for 2 h. The clear solution obtained was kept for slow evaporation, yielded white solid. The solid obtained was washed with warm ethanol: water mixture (1:1 v/v) and dried in a dessicator. Yield: 75%.

Anal. Cald. (%) for $C_{14}H_{14}LaN_7O_{11}$ (**4**): C, 28.25, H, 2.37, N, 16.47. Found, C, 28.23, H, 2.35, N, 16.44. ^{1}H-NMR (DMSO-d_6, 400 MHz, ppm): δ = 4.265 – 4.485 (m, 2H), 7.261 – 7.302 (q, 2H), 7.762 – 7.766 (td, 1H,), 9.268 – 9.313 (dt, 1H). FT-IR (KBr disc, cm^{-1}): ν = 3298 (N–H), 1660 (C=O), 1518 (C=N), 1480 and 1319 (NO_3^-, coordinated), 1384 (NO_3^-, ionic), 404 (La–O). λ_{max} (DMF/Tris-HCl) 234.95 nm (ε = 12,633 M^{-1} cm^{-1}), 260.34 nm (ε = 11,720 M^{-1} cm^{-1}). Λ_M (DMF, S cm^2 M^{-1}): 117.05.

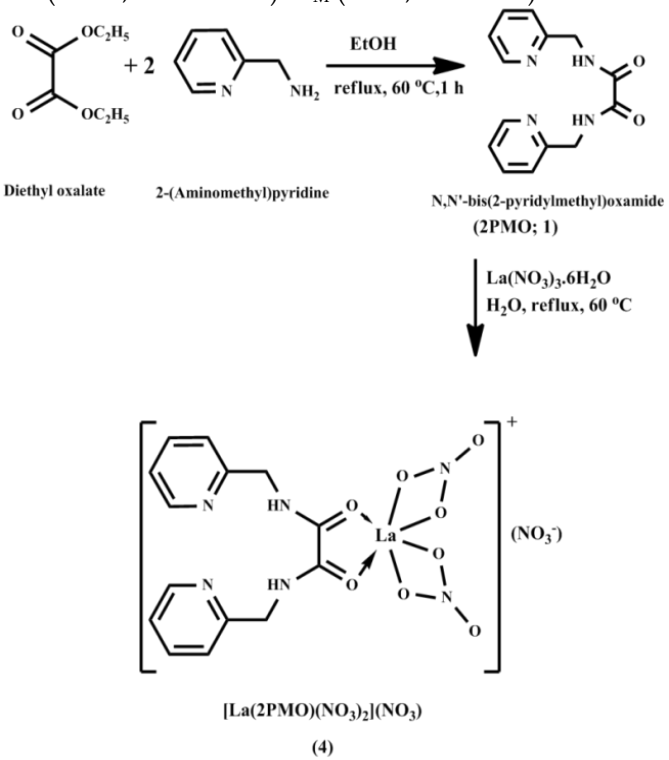

Scheme 1: Proposed synthetic route of [La(2PMO)(NO$_3$)$_2$](NO$_3$) (4).

The concept of "complexes as ligands" was used to synthesize binuclear complexes. [Cu(2PMO)] and [Ni(2PMO)] were used as "complex as ligands". A solution of 1,10-phenanthroline (0.2 mM, 0.040 g, 10 mL) in ethanol was stirred constantly. To this an aqueous solution of $La(NO_3)_3.6H_2O$ (0.2 mM, 120 mg, 15 mL) was added dropwise with continued stirring. Then aqueous solutions of [Cu(2PMO)] (0.2 mM, 0.066 g, 10 mL for **5**) and [Ni (2PMO)] (0.2 mM, 0.060 g, 10 mL for **6**) were added respectively in dropwise and stirring was continued for further 6 h. The resulting solutions were filtered. Dark green solid (**5**) and brown solid (**6**) were obtained on slow evaporation of the respective solutions. The solids were washed with ethanol: water (1:1 v/v) mixture and dried in a dessicator. Yield: 68% (**5**); 76% (**6**) (**Scheme 2**).

Anal. Cald. (%) for $C_{26}H_{20}CuLaN_9O_{11}$ (**5**): C, 37.31, H, 2.41, N, 15.06. Found, C, 37.29, H 2.39, N, 15.02. 1H-NMR (DMSO-d_6, 400 MHz, ppm): δ = 4.209 – 4.488 (d , 3H,) 7.295 – 7.788 (m , 4H), 8.260 – 8.637 (m, 2H), 9.307 – 9.457 (d, 1H). FT-IR (KBr disc, cm^{-1}): 1664 (C=O), 1520 (C=N), 1484 and 1318 (NO_3^-, coordinated), 1389 (NO_3^-, ionic), 402 (La–O), 494 (Cu–N). λ_{max} (DMF/Tris-HCl): 230.30 nm (ε = 13,366 M^{-1} cm^{-1}), 260.08 nm (ε = 7,766 M^{-1} cm^{-1}). Λ_M (DMF, S cm^2 M^{-1}): 145.65.

Anal. Cald. (%) for $C_{26}H_{20}NiLaN_9O_{11}$ (**6**): C, 37.53, H, 2.42, N, 15.15. Found, C, 37.51, H 2.40, N, 15.12. ^{1}H-NMR (DMSO-d_6, 400 MHz, ppm): δ = 4.199 – 4.434 (d, 3H), 7.262 – 7.872 (m, 4H), 8.416 – 8.626 (m, 2H), 9.287 – 9.298 (d, 1H). FT-IR (KBr disc, cm^{-1}): 1666 (C=O), 1519 (C=N), 1489 and 1312 (NO_3^-, coordinated), 1382 (NO_3^-, ionic), 401 (La–O), 491 (Cu–N). λ_{max} (DMF/Tris-HCl): 230.58 nm (ε = 13,367 M^{-1}cm^{-1}), 260.08 nm (ε = 10,333 M^{-1}cm^{-1}). Λ_M (DMF, S cm^2 M^{-1}): 149.64.

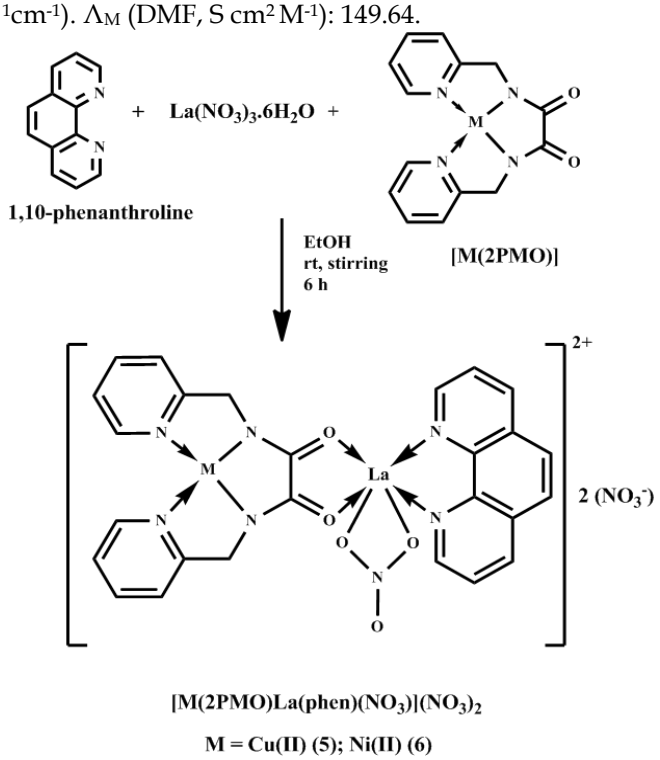

Scheme 2. Proposed synthetic route of [M(2PMO)La(phen)(NO$_3$)](NO$_3$)$_2$. M = Cu (5); Ni (6).

General Methods

The elemental analyses of carbon, hydrogen and nitrogen of the newly synthesized La(III) mononuclear (**4**) and binuclear complexes (**5** and **6**) were carried out using a Thermo Finnigan FLASH EA 1112 CHNS analyzer. ^{1}H NMR spectra of the complexes were recorded on 400 MHz liquid state Bruker NMR spectrometer obtained in DMSO-d_6 solution at approximately 25°C using tetramethyl silane (TMS) as internal standard. The IR spectra of the ligand and complexes were recorded using KBr pellets over the region 4000–400 cm^{-1} on a Shimadzu FT-IR spectrophotometer. UV-Visible absorption spectra of

the ligand and complexes were recorded on SpectraMax Plus 384 spectrophotometer. 10^{-3} M solutions of the ligand and complexes were prepared in DMF solvent and recorded in the wavelength ranging from 200 to 800 nm. The time-dependent stability of the complexes **4-6** in solution state were measured upto 6 h at pH = 7.2, 25 ˚C in DMF/Tris-HCl buffer by UV-Visible absorption spectroscopy using SpectraMax Plus 384 spectrophotometer. Full scan mass spectra (ESI-MS) of the complexes were recorded in positive ion mode on Shimadzu-LCMS equipped with APCI and ESI probes. The corresponding m/z values were recorded in the expected range. Conductivity measurements were carried out using 10^{-3} M solutions in DMF on Control Dynamics (India) conductivity meter with a dip-type cell, calibrated with a (0.1 M) solution of AnalaR potassium chloride. The molar conductivity values were used to determine the electrolytic nature of the complexes. Electrochemical experiments were performed on a CHI 600E Electrochemical analyzer controlled by PC. The cyclic voltammograms of 10^{-3} M solutions of ligand and binuclear complexes in DMF solvent were recorded in the potential range of -0.4 V to 0.7 V at the scan rate of 25 – 200 mV s^{-1} at 25˚C using 0.1 M tetra butyl ammonium perchlorate (TBAP) as supporting electrolyte. The three-electrode configuration was made up of glassy carbon as the working electrode, standard calomel electrode (SCE) as reference electrode and platinum wire as auxiliary electrode. Prior to each measurement, the working electrode and auxiliary electrodes were cleaned and polished with solid alumina of 1.0 µ, 0.5 µ and 0.05 µ respectively. The ligand and complex solutions were degassed with N2 atmosphere for 10 min prior to the electrochemical measurements.

DNA Interaction Studies

The ability of the newly synthesized complexes **4-6** in comparison with mononuclear complexes **2-3** and the ligand 2PMO (**1**) to interact with nucleic acid (DNA) is studied by their binding interactions with CT-DNA and cleaving ability towards SC pUC 19 DNA.

DNA binding experiments

UV-Visible absorption titrations

UV-Visible absorption titration experiment was carried out to study the interaction of La(III) complexes with CT–DNA. Absorbance was measured at 260 and 280 nm for CT-DNA in 5mM Tris-HCl buffer (pH = 7.2) gave the ratio of 1.9:1, indicating the DNA was free of protein. The intensity of the absorbed band at 260 nm with a known ε value (6600 $M^{-1}cm^{-1}$) was used to calculate the concentration of CT-DNA. [37] The absorption titrations were carried out at constant concentration of the complexes (30 µM) whereas concentration of CT-DNA was varied. Stock solutions (10^{-3} M) of complexes **2-6** were prepared by dissolving the complexes in DMF and diluted further to 30 µM using 5mM Tris-HCl buffer. The absorbance of DNA while measuring the spectra was eliminated by adding equal amounts of DNA to both complex and reference solutions. The complex solution was allowed to get equilibrated for 5 mins after the addition of known aliquots of CT-DNA solution to allow the complex to bind to the DNA. [31] The changes in the absorption intensities were monitored at regular intervals and used to calculate the intrinsic equilibrium binding constant (K_b) values by McGhee-von Hippel (MvH) method using the following equation. [38]

$$(\varepsilon_a-\varepsilon_b)/\ (\varepsilon_b-\varepsilon_f)= (b-(b^2-2K_b^2C_t[DNA]/s)^{1/2})/2K_bC_t$$

Where b is $(1+K_bC_t+K_b\ [DNA]/2s)$, ε_a is the extinction coefficient observed for the charge transfer absorption band at a given concentration of DNA, ε_f is the extinction coefficient observed for the absorption band of the complex in the absence of DNA, ε_b is the extinction coefficient of the complex in fully bound form with DNA, K_b is the intrinsic equilibrium constant, C_t is the total concentration of the metal complex in solution, [DNA] is the concentration of DNA in nucleotides and *s* is the binding site size in base pairs. The non-linear least square analyses were carried out using the software Origin Lab, version 6.1. [39]

Electrochemical titrations - Cyclic voltammetry

The mode of interaction of the ligand 2PMO (**1**) and the complexes **2-6** with CT-DNA were further confirmed by carrying out electrochemical experiments. [40] Cyclic voltammetric measurements were recorded using glassy carbon as working electrode, saturated calomel as reference electrode and platinum wire as auxiliary electrode. All the measurements were recorded using Tris-HCl (5 mM)/NaCl (50 mM) buffer (pH = 7.2) as supporting electrolyte at 25 ˚C. The reaction solutions were degassed in N_2 atmosphere for 10 mins before carrying out the experiment. The redox behavior of the 30 µM 2PMO (**1**) and the complexes **2-6** were studied in the absence and presence of CT-DNA (90 µM) at the scan rate of 25 mV s^{-1} to 200 mV s^{-1} in the potential range -0.4 to 0.7 V. The cyclic voltammetric experiment was also carried out to study the binding nature of 2PMO (**1**) and the complexes **2-6** at constant concentration (30 µM) with increasing concentration of CT-DNA at the scan rate of 200 mVs^{-1} in the potential range of -0.4 to 0.7 V. The shift in the peak potential values indicates the mode of interaction of the ligand and complexes with CT-DNA. The formal potentials of the ligand and complexes in the free form ($E_f^{0\prime}$) and fully bound form ($E_b^{0\prime}$) were used to calculate the binding constant ratios using the following formula:

$$E_b^{0\prime}-E_f^{0\prime} = 0.0591 \log [K_R/K_O)]$$

Where K_R/K_O is the ratio of binding constants of the complexes in the reduced form to the oxidized form.

Viscosity measurements

Viscometric titrations were carried out using Micro-Ubbelohde Viscometer which was thermo-stated at 37°C in a constant temperature bath. The concentration of CT-DNA was kept constant (150 µM, NP) while concentration of complex solutions were increased at regular aliquots. The flow times were measured with automated times and each sample was measured three

times for accuracy and average time flow was calculated for each complex solution. A graph of $(\eta/\eta_0)^{1/3}$ vs. [complex]/ [DNA] was plotted where η is the viscosity of CT-DNA in the presence of complex solution and η_0 is the viscosity of CT-DNA alone. Viscosity values were calculated using observed flow times of DNA containing solutions (t) corrected to that of buffer alone (t_0). [41]

$$\eta = (t - t_0) / t_0$$

DNA cleavage studies

Chemical nuclease activity – Pilot experiment

The agarose gel Electrophoresis method was used to determine the ability of the 2PMO (**1**) and the complexes **2-6** to cleave super coiled (SC) pUC 19 DNA to the nick circular (NC) form. The gel electrophoresis was carried out using 16-toothed combed gel trays of 210-150 mm. A constant voltage of 60 V at 10 mA was supplied using an Electrophoresis Power Supply Bangalore-Genei (India) system during electrophoresis. The cleavage experiment was carried out using SC pUC19 DNA (33.3 µM, 2 µg, NP) in 50mM Tris-HCl/50 mM NaCl (pH = 7.2). The concentration of the ligand and complexes were corresponding to the final volume of the reaction mixture in the gel-well. The band intensities were used to measure the extent of cleavage of SC pUC 19 DNA using UVITEC Gel Documentation System. Due corrections were made for the low level of nicked circular (NC) form present in the original super coiled (SC) DNA sample and for the low affinity of EB binding to SC compared to NC and linear forms of DNA. [42]

Chemical nuclease activity – Mechanistic studies

Mechanistic studies were carried out to study the involvement of free radicals in the oxidative cleavage of SC pUC 19 DNA by complexes. Agarose gel electrophoresis was carried out in the presence of radical quenchers such as DMSO which inhibit hydroxyl radicals and sodium azide (NaN_3) which inhibits singlet oxygen. Methyl green, a major groove binder was used to study the site of binding of hetero binuclear La(III) complexes **5** and **6** (10 µM) during oxidative cleavage. [43]

Antibacterial activities

The antibacterial properties of the ligand 2PMO (**1**) and its complexes **2-6** were determined by following standard protocol of Agar disc diffusion method. [44-45] The test organisms *Escherichia coli*, *Klebsiella pneumonia*, *Bacillus subtilis* and *Staphylococcus aureus* were maintained on nutrient agar slants overnight. The bacterial cultures were then centrifuged at 8000 rpm for 10 min. The bacterial cells were suspended in saline to make a suspension of 10^5 CFU/ mL and used for assay. The bacterial culture was then spread over the nutrient agar plate using sterile swab and the petri plates were allowed to dry. The test samples 2PMO (**1**) and its complexes (**2-6**) were dissolved in DMSO (1 mg mL^{-1}). The discs were prepared from Whatman filter paper and had been impregnated with DMSO solutions of 2PMO (**1**) and its complexes (**2-6**) respectively were placed on agar surface. Each test plate consists of one standard antibiotic tetracycline (30 µg mL^{-1}) and the other test samples (50 µg mL^{-1} and 100 µg mL^{-1}). The discs were placed equidistant to one another. The plates were then incubated at 37°C for 24 h. After incubation, the plates were checked for zone of inhibition. The inhibition zones were measured and compared with the standard, tetracycline. DMSO was used as negative control.

Antioxidant activities

The antioxidant activities of synthesized 2PMO (**1**) and its complexes (**2-6**) were tested by DPPH free radical scavenging method and ferrous ion chelating activity.

DPPH free radical scavenging activity

The most widely used method to check the antioxidant activity is the DPPH radical scavenging activity method. DPPH being a stable nitrogen based free radical gives violet colour in its oxidized form, changes to yellow colour on reduction either by electron transfer or hydrogen transfer. The compounds which facilitate this reaction are considered to be radical scavengers or antioxidants. DPPH has an absorbance of 517 nm in its radical form that disappears after accepting hydrogen radical or electron from the antioxidant and becomes a stable diamagnetic substance. [46-47] The DPPH radical scavenging ability of the synthesized ligand 2PMO (**1**) and its complexes (**2-6**) were determined by modifying the method reported by Brand-Williams et al. [57] 1 mg mL^{-1} stock solutions were prepared by dissolving 2PMO (**1**) and its complexes (**2-6**) in DMF. Test solutions (10-70 µg mL^{-1}) were taken in 96-well plate and the volumes were made up to 200 µL using 5 mM Tris-HCl buffer (pH = 7.4). 200 µL of positive controls were prepared using Butylated hydroxy toluene (BHT) and Ascorbic acid (AA) in a manner exactly same as test samples. DPPH in ethanol (500 µM) was added to all the wells. The 96-well plate was then kept under dark for 30 min incubation. Blank solution contained same experimental solutions except that of test samples. Absorbance was then measured at 517 nm against the blank. The decrease in absorbance measures the radical scavenging ability of the complexes. Radical scavenging ability was expressed as %I i.e., the ability of complexes to scavenge DPPH radicals.

Ferrous ion chelating assay

Ferrozine has the ability to chelate Fe^{2+} ions resulting in red colour. When other chelating agents are present, the ferrozine- Fe^{2+} complex formation is disrupted and the red colour will be diminished. The decrease in the red colour formation is a measure of chelating ability of the chelating agents present and the decreased intensity is measured at 562 nm by UV-Visible spectrophotometer. The ability of the 2PMO (**1**) and its complexes (**2-6**) to chelate Fe^{2+} ions were determined by the reported methods with slight modifications. [48-49] 1 mg mL^{-1} stock solutions were prepared by dissolving 2PMO (**1**) and its complexes (**2-6**) in DMF. 10-70 µL from the stock solutions of the tested complexes were

added to a 96-well microplate and the volumes were made upto 150 µL using distilled water. To these wells, 2 mM $FeCl_2$ solution (20 µL) was added. The reaction was initiated by adding 5 mM Ferrozine (30 µL) to each well and shaken vigorously. The microplate was then incubated for 10 min at room temperature. Once the reaction mixture attained equilibrium, absorbance of each well was measured at 562 nm against the blank (reaction mixture without test samples). EDTA-Na_2 was used as standard. The reaction mixture without test sample is used as blank. The ferrous ion chelating ability (% inhibition of formation of ferrozine-Fe^{2+} complex) was calculated using the formula:

Ferrous ion chelating ability (%) = $[1- A_s/A_0] \times 100$

Where A_s is the absorbance in the presence of test sample and A_0 is the absorbance of blank. A graph using %I i.e., % inhibition of ferrozine-Fe^{2+} complex formation vs. concentration of sample were plotted. Using the graph, EC_{50}, the efficient concentration at which 50% of the metal chelation was occurred was calculated.

Cytotoxicity activities – MTT assay

The cytotoxic effects of 2PMO (**1**) and its La(III) complexes (**5** and **6**) were tested against human breast cancer cells (MCF-7) by 3-(4,5-dimethylthiazol-2-yl)-2,5-diphenyltetrazolium bromide (MTT) assay as per the reported procedure with slight modifications. [50-51] The assay of the test samples 2PMO (**1**) and its complexes (**5** and **6**) was carried out in the concentration range 10-320 µg mL^{-1}. MTT assay is a colorimetric assay based on the fact that 3-(4,5-dimethylthiazol-2-yl)-2,5-diphenyltetrazolium bromide (MTT) dye is a pale yellow substrate taken up by live cell mitochondria which is then reduced by mitochondrial oxidoreductase enzymes into an insoluble purple color formazan product. The cellular oxidoreductase enzymes may reflect the number of viable cells under given conditions. Briefly, MCF-7 cells (3×10^3 cells/well) in RPMI-1640 medium (supplemented with 10% FBS, 100 U/mL penicillin, 100 µg mL^{-1} streptomycin and 2 mM glutamine) with a final volume of 200 µL were seeded into 96-wells culture plate and incubated overnight at 37°C with the supply of 5% CO_2. The stock solutions of 2PMO (**1**) and its La(III) complexes (**5** and **6**) were prepared in DMSO of molecular biology grade and diluted to required concentrations using RPMI-1640 medium. The cells were treated with or without test samples of known concentrations and were incubated at 37°C with the supply of 5% CO_2 for 48 h. After incubation, the cells were washed with phosphate buffer saline (PBS). At the end of the treatment period, 20 µL MTT (5 mg mL^{-1}) was added to each well and incubated for 4 h at 37°C with the supply of 5% CO_2. After incubation, the blue formazan products formed in the cells were dissolved in DMSO (100 µL) and measured spectrophotometrically at 540 nm. The percentage cell viability of the complex untreated and treated cells were calculated and represented graphically.

Table 1: Physicochemical data of complexes 4-6.

	16	17	18
M. W.[a]	595.21	836.94	832.09
M. P.[b] (°C)	204	> 300	> 300
IR[c], cm^{-1} [ν(C=O)]	1660	1660	1666
λ[d], nm (ε, M^{-1} cm^{-1})	234.95 (12,633)	230.30 (13,366)	230.58 (13,367)
Λ_M[e], S cm^2 M^{-1}	117.05	145.65	149.64
$E_{1/2}$[f] (V)	-0.1233	-0.1122	-0.1073

[a] Molecular weight.
[b] Melting point
[c] IN KBr phase
[d] UV-Visible absorption band in DMF.
[e] Molar conductivity values in DMF.
[f] The formal potentials are vs. SCE. $E_{1/2}$ is the average of cathodic and anodic peak potentials.

RESULTS AND DISCUSSION

Syntheses

One mononuclear complex (**4**) and two binuclear complexes (**5-6**) are newly synthesized following literature method using *N,N'*-bis(2-pyridylmethyl)oxamide (2PMO) as ligand (**1**), [Cu(2PMO)] (**5**) and [Ni(2PMO)] (**6**) "complexes as ligands" concept under given conditions as in **Schemes 1-2**. All the newly synthesized complexes are characterized by ^{1}H-NMR, FT-IR spectroscopy, UV-Visible absorption spectroscopy, ESI-Mass spectrometry, molar conductivity measurement, electrochemical measurements and elemental analyses. The complexes are soluble in methanol, dichloromethane, DMF, DMSO and Tris-HCl buffer (pH = 7.2) and are highly stable in DMF/Tris-HCl buffer solutions. All the results are correlated and are in the expected range. Molar measurements reveal that newly synthesized complex **4** is 1:1 electrolyte whereas complexes **5** and **6** are 1:2 electrolytes in DMF solvent.

General Methods

^{1}H-NMR spectra reveal the presence of $-CH_2$ protons in the region 4.19 – 4.48 ppm in the all the newly synthesized complexes **4-6**. Complex **4** has chemical shift values around 7.76 – 7.77 ppm which correspond to –NH of amide protons. The aromatic protons appear around 7.26 – 7.87 ppm and 9.25 – 9.31 ppm which correspond to pyridyl group in complexes **4-6**. Complexes **5** and **6** have additional aromatic protons around 8.26 – 8.63 ppm, correspond to 1,10-phenanthroline. [7]

IR spectra reveals the presence of characteristic carbonyl (-C=O) peak of the oxamide ligand (2PMO) in all the complexes **4-6**. The oxamide –C=O appears at 1666 cm^{-1}, 1660 cm^{-1} and 1666 cm^{-1} in complexes **4**, **5** and **6** respectively. The ligand carbonyl peak at 1649 cm^{-1} has been shifted to higher frequencies in complexes **4-6**, reveal the coordination of the 2PMO ligand through –C=O. When oxamide coordinates through –C=O, the –N–C–O vibrations have been shifted to higher frequencies as in protonated species. This confirms the coordination of oxamide through –

C=O bond. The –NH group is deprotonated and coordinated to d-metal ion and hence the secondary –NH peak is absent in IR spectra of complexes **5** and **6**. The secondary –NH peak appears at 3298 cm^{-1} in complex. The presence of coordinated NO_3^- peaks appear at 1480 and 1319 cm^{-1}, 1484 and 1318 cm^{-1} and 1489 and 1312 cm^{-1} in complexes **4**, **5** and **6** respectively are due to the ν_4 and ν_1 vibrations of the nitrate group of C_{2v} symmetry of the coordinated nitrate. The ionic nitrate appears at 1384 cm^{-1} in complex **4**, 1389 cm^{-1} in complex **5** and 1382 cm^{-1} in complex **6**. [52-53] The frequencies observed around 404 cm^{-1}, 402 cm^{-1} and 401 cm^{-1} in complexes **4**, **5** and **6** respectively are due to ν(La–O) [36] and the stretching bands ν(Cu–N) at 494 cm^{-1} in complex **5** and ν(Ni–N) 491 cm^{-1} in complex **6** confirms the coordination of oxamide through amide nitrogen with M(II) ion.

UV-Visible absorption spectra reveal the n → π* transitions of the oxamide –C=O at 234.95 nm, 232.58 nm and 233.30 nm in complexes **4**, **5** and **6** respectively. The π → π* transitions absorb at 262.8 nm, 260.08 nm and 260.08 nm in complexes **4**, **5** and **6** respectively. The n → π* transitions in complexes have been red shifted when compared with the ligand 2PMO (229.53) and the π → π* transitions show hyperchromism on complexation.

ESI-Mass spectra confirm the formation of ionic complexes. The m/z value that appeared for complex **4** at 583.05 in negative scan mode corresponds to [M+OH^-+CH_3OH– (NO_3^-)] where M = $[La(2PMO)(NO_3^-)_2]^+$ ion. Complex **5** has the m/z value at 425.11 in positive ion mode. This value corresponds to [M+Na+CH_3OH–2(NO_3^-)] where M = $[Cu(2PMO)La(phen)(NO_3)]^{2+}$ ion. Complex **6** has m/z value at 391.20 which is corresponding to [M+K–2(NO_3^-)] where M = $[Ni(2PMO)La(phen)(NO_3)]^{2+}$ ion.

The electrochemical responses of newly synthesized complexes in DMF were determined by using 0.1 M TBAP as supporting electrolyte at the scan rate of 200 mVs^{-1}. Complexes **4-6** have shown the change in reduction and oxidation peak potentials which is an indicative of the redox behavior of the complexes. [30] The formal potential values of new complexes **4-6** are given in **Table 1**.

DNA binding experiments

UV-Visible absorption titrations

Electronic absorption titrations were carried out to study the DNA binding propensities of the complexes **2-6** to the calf-thymus (CT) DNA in 5 mM Tris-HCl/50 mM NaCl buffer (pH = 7.2). The changes in the absorption intensities of the spectral bands of the complexes as a function of increased concentration of CT-DNA were determined (**Fig. 1**). The intrinsic binding constants (K_b) of the complexes to the CT-DNA were determined by monitoring changes in the spectral band with increasing CT-DNA concentration, keeping complex concentration constant (30 µM). The binding constant values were given in **Table 2**.

Table 2: UV-Visible absorption titration data of 30 µM complexes 2-6 in the presence of CT-DNA.

Complex	Empirical formula	K_b (M^{-1})	[*s*]
2	[Cu(2PMO)	$4.69 \times 10^4 \pm 0.76$	0.21 ± 0.0059
3	[Ni(2PMO)]	$3.12 \times 10^4 \pm 0.9$	0.20 ± 0.0053
4	$[La(2PMO)(NO_3)_2](NO_3)$	$8.53 \times 10^4 \pm 0.2$	0.23 ± 0.0046
5	$[Cu(2PMO)La(phen)(NO_3)](NO_3)_2$	$6.35 \times 10^5 \pm 0.1$	0.24 ± 0.0033
6	$[Ni(2PMO)La(phen)(NO_3)](NO_3)_2$	$4.93 \times 10^5 \pm 0.4$	0.22 ± 0.0067

K_b= intrinsic binding constant. [s]= site size in base pairs.

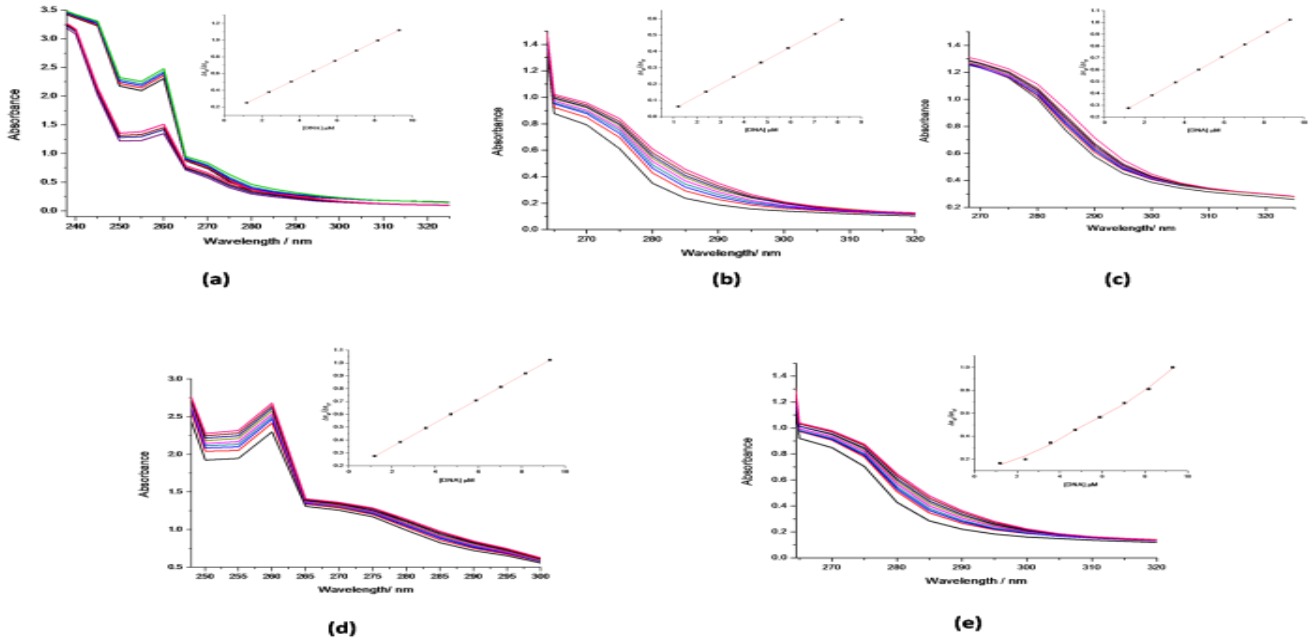

Fig. 1: UV-Visible absorption titration spectra (a–e) of complexes 2-6 (30 µM) respectively in the presence of increased amount of CT-DNA in 5 mM Tris-HCl/ 50 mM NaCl buffer (pH=7.2). The inset plots show $\Delta\varepsilon_{af}/\Delta\varepsilon_{bf}$ vs. [DNA]/ µM that used to calculate intrinsic binding constant K_b M^{-1}.

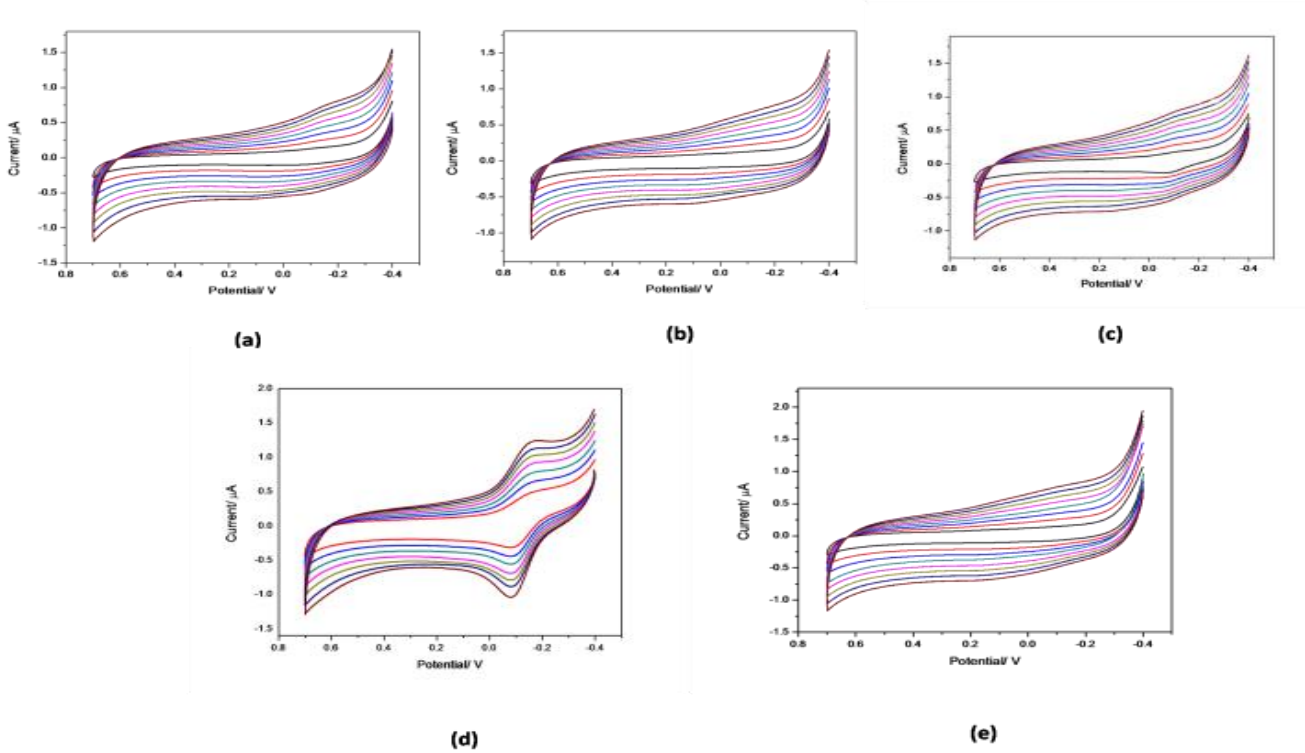

Fig. 2: Cyclic voltammograms of 2-6 (a-e) (30 µM) in the presence of CT-DNA (100 µM) in 5 mM Tris-HCl buffer (pH = 7.2) using 50 mM NaCl as supporting electrolyte in the potential range -0.4 to 0.7 V at the variable scan rate 25 – 200 mVs^{-1}.

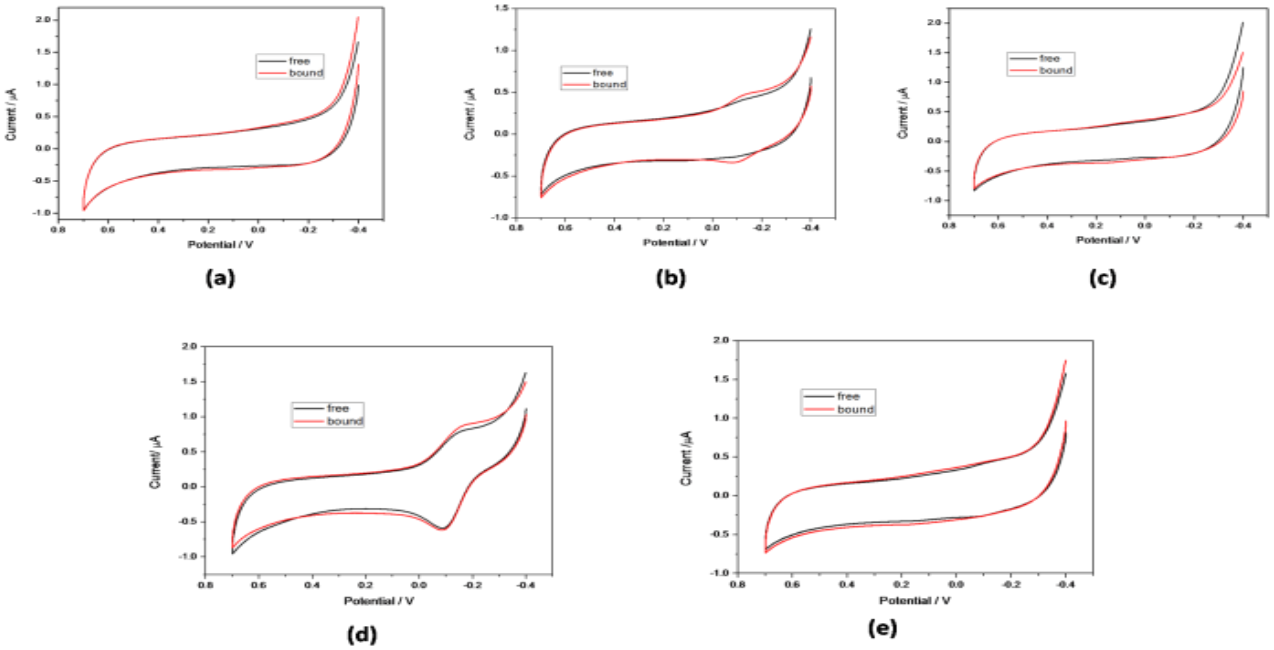

Fig. 3: Cyclic voltammograms of 2-6 (a-e) in free complex and complex fully bound with CT-DNA in 50 mM Tris-HCl buffer (pH = 7.2) using 50 mM NaCl as supporting electrolyte in the potential range -0.4 to 0.7 V at the scan rate 200 mVs^{-1} at room temperature.

From the **Fig. 1** it is observed that, on incremental additions of CT-DNA to the complex solutions, the absorption intensity decreases. The significant hypochromism and slight red shift are the characteristic spectral changes in the intercalative mode. This may be due to the coupling of π^*-orbital of the intercalated complex with that of π-orbital of the base pairs of DNA results in decreasing the π-π^* transition energy and hence bathochromic shift and hypochromism. [54-55] The binding strengths of the complexes follow the order: **5** > **6** > **4** > **2** > **3**. Among all the complexes [Cu(2PMO)La(phen)(NO_3)](NO_3)$_2$ (**5**) has shown the highest binding constant values.

Electrochemical titrations – Cyclic voltammetry

The mode of binding and the nature of complexes in binding towards CT-DNA are further confirmed by electrochemical titrations. The cyclic voltammetry is carried out in two ways. Firstly, the concentration of complexes **2-6** (30 µM) and the concentration of CT-DNA (100 µM) both are kept constant while varying the scan rate from 25 to 200 mV s^{-1}. Secondly, at the fixed scan rate 200 mV s^{-1}, electrochemical titrations were

carried out by keeping concentration of complex constant (30 µM) and the DNA was added in regular aliquots. The formal peak potential values in the absence ($E_f^{0\prime}$) and presence of CT-DNA ($E_b^{0\prime}$) were determined and changes in the voltammetric current were observed. The E_f^0 and E_b^0 values are given in the **Table 3**. The changes in the redox behavior of the complexes are shown in **Figs. 2** and **3.**

From the **Table 3** it is observed that, the peak potential values are shifted to positive potential and the voltammetric current decreases on addition of complexes to CT-DNA solution. The reason may be attributed to the fact that, once the complexes are bound to DNA through intercalation, the molecules diffuse more slowly into the electrolyte solution and hence voltammetric current decreases. The $E_f^{0\prime}$ and $E_b^{0\prime}$ values are used to calculate the ratio of binding constants of complexes in reduced state to the oxidized state and the results reveal that, all the complexes bind to CT-DNA in the reduced state.

Viscosity Method

The binding mode of the complexes to CT-DNA was further confirmed by viscosity method. Viscosity method is known to be the least ambiguous technique to determine the binding interaction of complexes in the absence of crystallographic data of the complexes. It is well known fact that, when crystallographic data is unavailable, viscosity method is the least ambiguous hydrodynamic method that is used to determine the binding mode of metal complexes with DNA. A classical intercalator intercalates between the base pairs of the DNA, thus increases the length of DNA helix and hence viscosity of DNA increases whereas partial or non-classical interaction of complex results in bending or kinking of DNA, thereby decreasing the length of the DNA and in turn decreases the viscosity of DNA. [41, 46, 55] The concentration dependent viscosity method reveals that, as the concentration of the complexes increases, viscosity of the DNA increases. The viscosity is highest for binuclear complexes (**5** and **6**) than their mononuclear analogues (**2-4**). This is due to the fact that the planar aromatic ring of 1,10-phenanthroline stabilizes the DNA-complex interaction through intercalation and hence the viscosity is increased. The change in the viscosity of CT-DNA in presence of complexes has been shown in **Fig. 4.**

DNA cleavage studies

The ability of the complexes **2-6** in comparison with the ligand 2PMO (**1**) to cleave super coiled (SC) pUC19 DNA in the absence and presence of oxidizing agent H_2O_2 and reducing agent MPA was studied by agarose gel Electrophoresis in 50 mM Tris-HCl buffer/50 mM NaCl (pH = 7.2). Of all the complexes and ligands studied, at 10 µM, complexes **5** and **6** have shown the maximum cleavage (92% and 88% respectively) in presence of reducing agent MPA as shown in **Fig. 5**. The SC pUC 19 DNA cleavage data in hydrolytic and oxidative conditions are given in **Table 4**. The mononuclear complexes **2-4** have shown poor chemical nuclease activity at the same concentration.

Table 3: Cyclic voltammetric data of complexes 2-6 in free form and fully bound with CT-DNA.

Complex	E_f (V)	I_c (µA)	E_b (V)	I_a (µA)	$E_f^{0\prime}$ (V)	$E_b^{0\prime}$(V)	K_R/K_O
2	-0.244	-1.42	-0.204	-2.78	-0.122	-0.102	2.17
3	-0.101	-1.26	-0.084	-1.62	-0.050	0.042	1.43
4	0.0798	-2.08	0.1368	-3.19	0.0399	0.0684	3.02
5	-0.081	-1.57	-0.068	-3.55	-0.041	-0.034	1.28
6	-0.088	-4.65	-0.084	-4.82	-0.044	-0.042	1.08

E_f = Electrode potential of free complex, E_b = Electrode potential of complex bound to DNA.

Table 4: SC pUC 19 DNA cleavage data of 2PMO (1) and its complexes 2-6.

Lanes	Reaction Conditions	% SC	% NC
1	DNA + NaCl + Tris-HCl	99	01
2	DNA + NaCl + Tris-HCl + H_2O_2	98	02
3	DNA + NaCl + Tris-HCl + MPA	97	03
4	DNA + NaCl + Tris-HCl + 1	98	02
5	DNA + NaCl + Tris-HCl + 1 + H_2O_2	98	02
6	DNA + NaCl + Tris-HCl + 1 + MPA	97	03
7	DNA + NaCl + Tris-HCl + 2	94	06
8	DNA + NaCl + Tris-HCl + 2 + H_2O_2	92	08
9	DNA + NaCl + Tris-HCl + 2 + MPA	70	30
10	DNA + NaCl + Tris-HCl + 3	97	03
11	DNA + NaCl + Tris-HCl + 3 + H_2O_2	98	02
12	DNA + NaCl + Tris-HCl + 3 + MPA	80	20
13	DNA + NaCl + Tris-HCl + 4	97	03
14	DNA + NaCl + Tris-HCl + 4 + H_2O_2	94	06
15	DNA + NaCl + Tris-HCl + 4+ MPA	84	16
16	DNA + NaCl + Tris-HCl + 5	97	03
17	DNA + NaCl + Tris-HCl + 5+ H_2O_2	87	13
18	DNA + NaCl + Tris-HCl + 5 + MPA	08	92
19	DNA + NaCl + Tris-HCl + 6	94	06
20	DNA + NaCl + Tris-HCl + 6 + H_2O_2	89	11
21	DNA + NaCl + Tris-HCl + 6+ MPA	12	88

[Complex]= 10 µM; [H_2O_2]= 200 µM; [MPA]= 500 µM; Tris-HCl/NaCl= 50 mM.

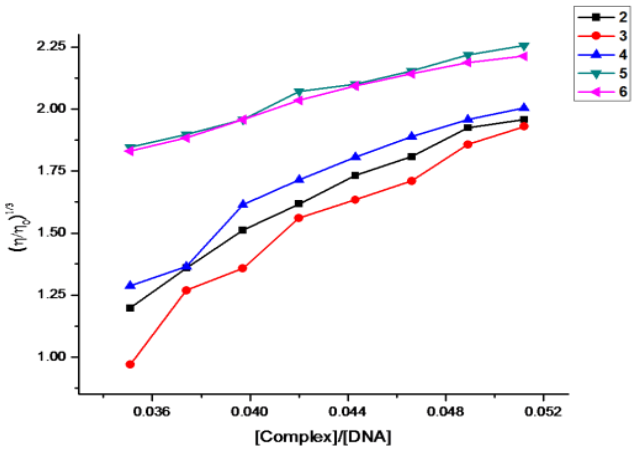

Fig. 4: A plot of [Complex]/[DNA] vs. $(\eta/\eta_0)^{1/3}$ showing the change in viscosity of CT-DNA with increasing concentration of complexes 2-6 in the presence of 50 mM Tris-HCl/NaCl buffer (pH = 7.2) at 37°C.

The oxidative cleavage is mediated by the generation of diffusible free radicals by metal complexes. The involvement of highly reactive oxygen species such as hydroxyl radicals or singlet oxygen in cleaving SC pUC 19 DNA by complexes **5** and **6** were determined by the mechanistic studies carried out by agarose gel electrophoresis in presence of reducing agent MPA

using radical quenchers DMS and sodium azide (NaN_3) and major groove binder methyl green. No significant inhibition of cleavage is observed in presence of singlet oxygen quencher NaN_3 whereas cleavage activity is inhibited in presence of hydroxyl radical quencher DMSO and major groove binder MG. This confirms that the complexes **5** and **6** intercalate between the DNA base pairs in the major groove direction. The results are shown in **Fig. 6** and the cleavage data is given in **Table 5.**

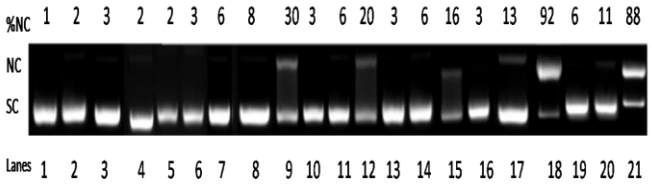

Fig. 5: Agarose gel electrophoretic diagram showing the cleavage of SC pUC 19 DNA by 2PMO (1) and its complexes 2-6 (10 µM) in presence of 50 mM Tris-HCl/ NaCl buffer (pH = 7.2), oxidizing agent H_2O_2 and reducing agent MPA. Lane 1, DNA alone; lane 2, DNA + H_2O_2; lane 3, DNA + MPA, lane 4, DNA + 1; lane 5, DNA + H_2O_2 + 1; lane 6, DNA + MPA + 1; lane 7, DNA + 2; lane 8, DNA + H_2O_2 + 2; lane 9, DNA + MPA + 2; lane 10, DNA + 3; lane 11, DNA + H_2O_2 + 3; lane 12, DNA + MPA + 3; lane 13, DNA + 4; lane 14, DNA + H_2O_2 + 4; lane 15, DNA + MPA + 4; lane 16, DNA + 5; lane 17, DNA + H_2O_2 + 5; lane 18, DNA + MPA + 5; lane 19, DNA + 6; lane 20, DNA + H_2O_2 + 6; lane 21, DNA + MPA + 6.

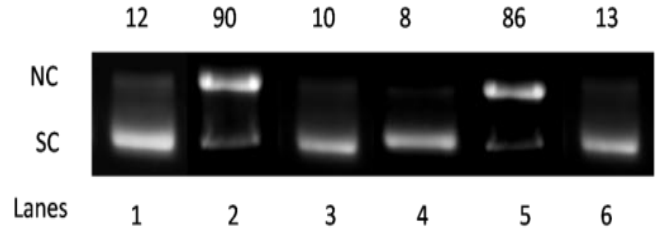

Fig. 6: Agarose gel electrophoretic diagram showing the cleavage of SC pUC 19 DNA by complexes 5 and 6 in the presence of additives like DMSO, NaN_3 and methyl green (MG) in 50 mM Tris-HCl/NaCl buffer (pH = 7.2). Lane 1, DNA + MPA + 5 +DMSO; lane 2, DNA + MPA + 5 + NaN_3; lane 3, DNA + MPA + 5 + MG; lane 4, DNA + MPA + 6 + DMSO; lane 5, DNA + MPA + 6 + NaN_3; lane 6, DNA + MPA + 6 + MG.

Table 5: SC pUC 19 DNA cleavage data of mechanistic studies of 5 and 6 in presence of DMSO, NaN_3 or MG at 10 µM.

Lane no.	Reaction Conditions	%SC	%NC
1	DNA + NaCl + Tris-HCl + MPA + 5 + DMSO	88	12
2	DNA + NaCl + Tris-HCl +MPA + 5 + NaN_3	10	90
3	DNA + NaCl + Tris-HCl +MPA + 5+ MG	90	10
4	DNA + NaCl + Tris-HCl +MPA + 6 + DMSO	92	8
5	DNA + NaCl + Tris-HCl + MPA + 6 + NaN_3	14	86
6	DNA + NaCl + Tris-HCl + MPA + 6 + MG	87	13

[MPA] = 500 µM, DMSO = 4 µL, [NaN_3] = 200 µM, Methyl green (MG) = 10 µM, [Complex] = 10 µM.

Thus it can be proposed that in presence of MPA, Cu(II) reduces to Cu(I) and Ni(II) to Ni(I) and in turn activate the molecular oxygen into hydroxyl radical which is responsible for the cleavage of SC pUC 19 DNA. [57]

Based on the above observation, a mechanism for the cleavage of SC pUC19 DNA by complexes **5** and **6** in the presence of MPA can be proposed (**Scheme 3**).

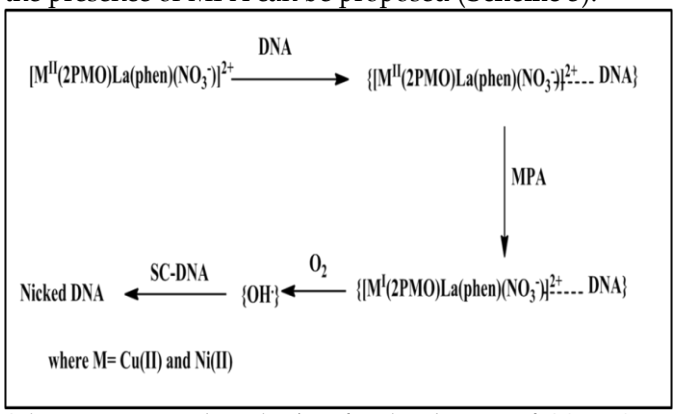

Scheme 3. Proposed mechanism for the cleavage of SC pUC 19 DNA by complexes 5 and 6 in the presence of MPA mediated by hydroxyl radicals.

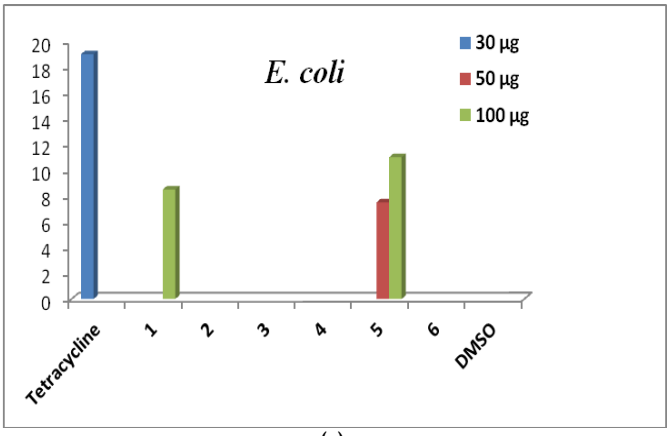

(a)

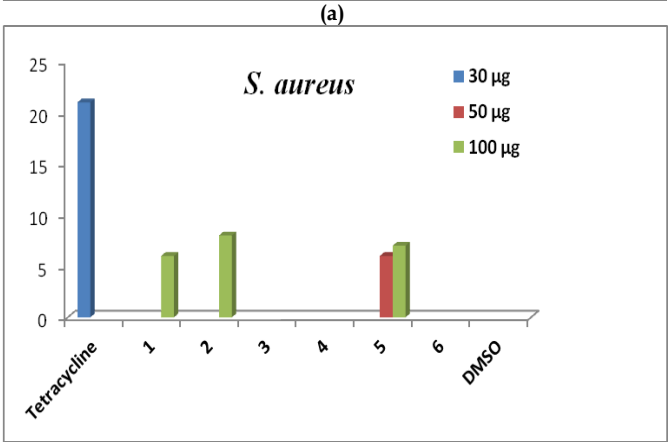

(b)

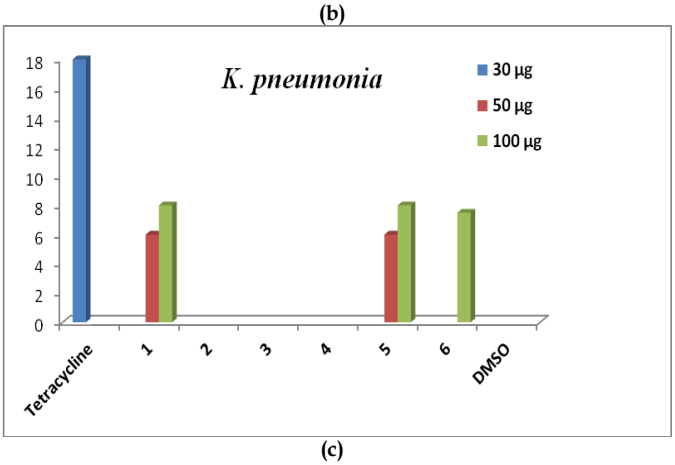

(c)

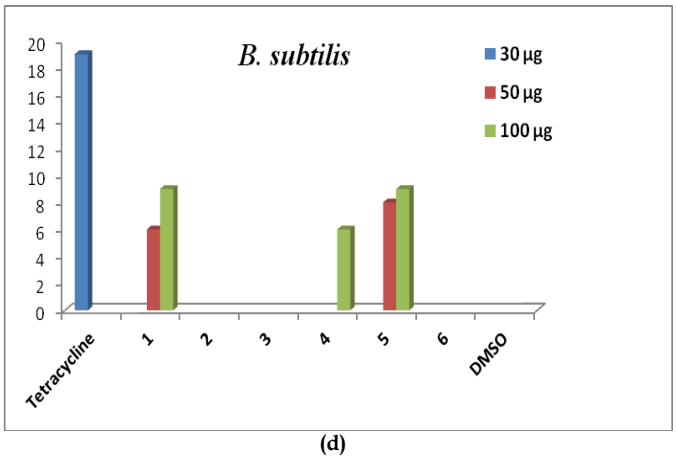

(d)

Fig. 7: Bar diagrams showing zone of inhibition of growth of (a) *E. coli*, (b) *S. aureus*, (c) *K. pneumonia* and (d) *B. subtilis* by 2PMO (1) and its complexes (2-6).

Antibacterial studies

The antibacterial activities of the ligand 2PMO (**1**) and its mononuclear (**2-4**) as well as binuclear complexes (**5-6**) are determined by Agar disc diffusion method against Gram negative bacteria (*E. coli* and *K. pneumonia*) and Gram positive bacteria (*B. subtilis* and *S. aureus*). From the **Fig. 7** it can be observed that at 50 µg mL^{-1}, only complex **5** is active against all the four tested bacteria. At 100 µg mL^{-1}, 2PMO (**1**) is active only against *S. aureus*, complex **4** is active only against *B. subtilis* and complex **6** is active only against *K. pneumonia*. The antibacterial activity of the complexes can be explained on the basis of Tweedy's chelation theory. Coordination of oxamide –C=O with La(III) ion and N donor atoms of 1,10-phenanthroline reduces the polarity of the metal ion as the positive charge is shared by the ligand atoms. This enhances the lipophilicity of the complexes that favors the complexes to be permeable towards the lipid membranes of bacterial cell wall. Once the permeability of the bacterial cell wall is broken down, their normal physiology would be disturbed as their enzyme metabolism is affected and thus inhibits bacterial growth. [9-10]

Antioxidant studies

The ability of the newly synthesized complexes (**4-6**) in comparison with the ligand and mononuclear complexes (**1-3**) in scavenging free radicals are determined by the well known methods DPPH radical scavenging method and ferrous ion chelation method.

DPPH radical scavenging method

The ability of the tested complexes to scavenge DPPH radicals are compared with one natural antioxidant (ascorbic acid; AA) and one synthetic antioxidant (Butylated hydroxyl toluene; BHT). From the results (**Fig. 8**) it is observed that complex **4** shows better DPPH radical scavenging ability than the corresponding ligand and other mononuclear and binuclear complexes but not as good as standards. The antioxidant activity of this complex may be due to its electron releasing property of the -CH_2 groups or hydrogen-donating –NH groups present in the complex. [49]

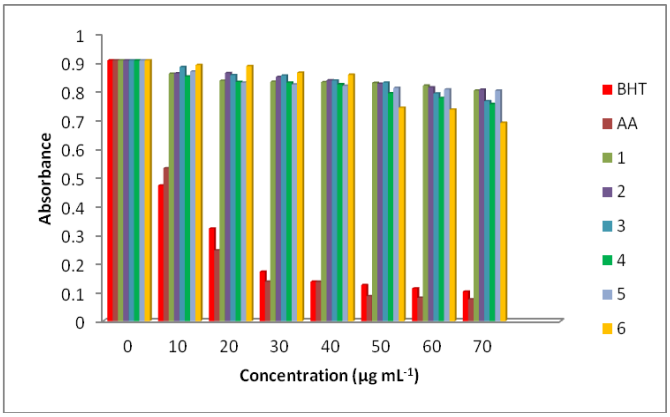

(a)

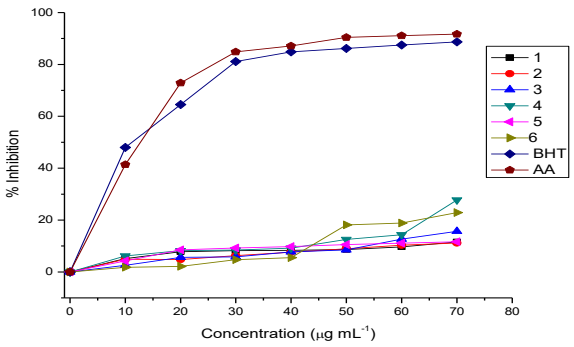

(b)

Fig. 8: (a) Bar diagram showing DPPH radical scavenging abilities of 1-6 in comparison with BHT and ascorbic acid (AA). (b) The plot of % Inhibition of formation of DPPH radicals vs. concentration (µg mL^{-1}) of complexes and standards BHT and AA.

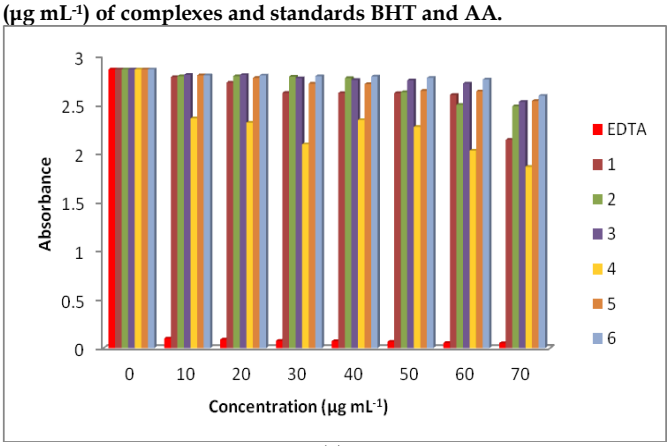

(a)

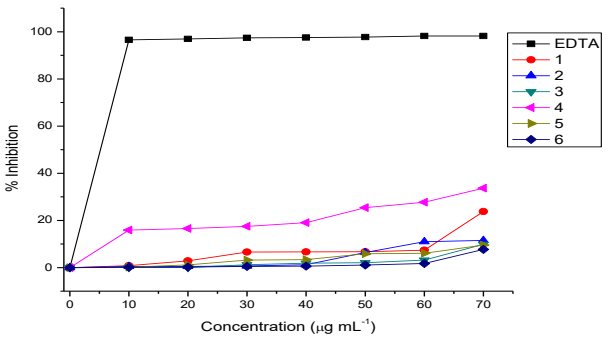

(b)

Fig. 9: (a) Bar diagram showing inhibition of Fe^{2+}-ferrozine complex formation by 1-6 in comparison with standard EDTA. (b) The plot of % Inhibition of formation of Fe^{2+}-ferrozine complex vs. concentration (µg mL^{-1}) of complexes and standard EDTA.

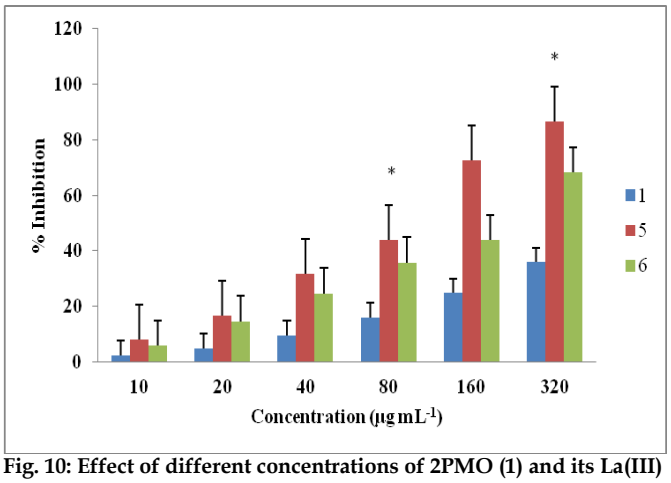

Fig. 10: Effect of different concentrations of 2PMO (1) and its La(III) complexes (5 and 6) on the viability of MCF-7 cells. The cells were treated with or without tested samples of different concentrations (10–320 µgmL^{-1}) on 96-well plate MTT assay. Values are significantly different from control if *P<0.05, using student t-test. The results are shown as a representative of three independent experiments.

Ferrous ion chelation method

The complexes are also tested for their ability to inhibit the formation of Fe^{2+}-ferrozine complex. From the results it is observed that, of all the complexes studied, only ligand (**1**) and complex **4** have shown better activity. Ligand **1** and complex **4** are showing better activity when compared with other complexes may be due to the availability of coordination sites in the oxamide pocket. The % inhibition shown by ligand **1** and complex **4** are found to be 23.76% and 33.65% respectively at 70 µg mL^{-1} but the activity is not as good as the standard used EDTA-Na_2 (**Fig. 9**).

Cytototoxicity activities – MTT assay

Evaluation of cytotoxic activities against cancerous cell lines is of great importance in developing potent anti-cancer agents. The *in vitro* cytotoxic activity of ligand (**1**) and the binuclear complexes (**5** and **6**) are carried out against MCF-7 cancer cell lines by MTT assay in the concentration range 10 - 320 µg mL^{-1}. Experimental results are shown in **Fig. 10** as a bar diagram. Results were expressed as % viability of cells compared to control (mean ± SD, n = 3). Values are significantly different from control if *P< 0.05, using student t-test. The results are shown as a representative of three independent experiments.

Experimental results reveal that, complexes **5** and **6** have shown better cytotoxic effect than their ligand 2PMO (**1**). The IC_{50} values are 118.3 µg mL^{-1} and 179.5 .µg mL^{-1} for complexes **5** and **6** respectively. From the results it can be explained that, 1,10-phenanthroline being classical intercalator induces the complexes **5** and **6** to penetrate through the cell membrane and intercalates between the base pairs of DNA, thereby inhibit the proliferation of the tumor cells. The cytotoxic activities of the complexes can be correlated to their ability to bind and cleave DNA. [61] Thus, it can be hypothesized that the hetero-binuclear La(III) complexes containing oxamide and planar aromatic heterocyclic rings can be used as potent anticancer agents**.**

Thus, on the basis experimental results it can be concluded that, the newly synthesized hetero-binuclear complexes [Cu(2PMO)La(phen)(NO_3)](NO_3)$_2$ (**5**) and [Ni(2PMO)La(phen)(NO_3)](NO_3)$_2$ (**6**) represent new class of pharmaceutical agents in possessing DNA binding ability, chemical nuclease property, antibacterial, antioxidant and cytotoxic abilities.

ACKNOWLEDGEMENTS

The authors greatly acknowledge the financial support received from the Department of Science and Technology (DST, SR/S5/BC-14/2006), Government of India, the University Grants Commission (UGC, Ref. No. F. No.39-754/2010(SR), DST-FIST and UGCSAP.

REFERENCES

1. Gao F, Yin C, Yang P, Coordination chemistry mimics of nuclease-activity in the hydrolytic cleavage of phosphodiester bond. Chin. Sci. Bull. 2004; 49: 1667-1680.
2. Rao R, Patra AK, Chetana PR, DNA binding and oxidative cleavage activity of ternary (L-proline)copper(II) complexes of heterocyclic bases. Polyhedron. 2007; 26: 5331–5338.
3. Li XW, Tao L, Li YT, Wu ZY, Yan CW. Bimetallic complexes constructed from asymmetrical N,N′-bis (substituted)-oxamide: Cytotoxicities, and reactivities towards DNA and protein Eur. J. Med. Chem. 2012; 54: 697-708.
4. Zhao FJ, Zhao HQ, Liu F, Li YT, Wu ZY, Yan CW. Synthesis and crystal structure of new dicopper(II) complexeswith N,N′-bis-(dipropylenetriamine)oxamide as bridging ligand: Effects of the counterions on DNA/protein-binding property and in vitro antitumor activity. J. Photochem. Photobio. B. 2015; 143. 148-162.
5. Xu XW, Li XJ, Zhu L, Li YT, Wu ZY, Yan CW. Synthesis and structure of dicopper(II) complexes bridged by N-(5-chloro-2-hydroxyphenyl)-N′-[3-(methylamino)propyl] oxamide: Evaluation of DNA/protein binding, DNA cleavage, and in vitro anticancer activity. J. Photochem. Photobio. B. 2015; 147: 9-23.
6. Zheng K, Zhu L, Li YT, Wu ZY, Yan CW. Synthesis and crystal structure of new dicopper(II) complexes having asymmetric N,N′-bis(substituted)oxamides with DNA/protein binding ability: In vitro anticancer activity and molecular docking studies. J. Photochem. Photobio. B: Biol. 2015; 149: 129-142.
7. Gupta T, Dhar S, Nethaji M, Chakravarty AR, Bis(dipyridophenazine)copper(II) complex as major groove directing synthetic hydrolase. Dalton Trans. 2004; 1896-1900.
8. Adjimani JP, Asare P. Antioxidant and free radical scavenging activity of iron chelators. Toxicol. Reports. 2015; 2: 721-728.
9. Badwaik VB, Aswar AS. Synthesis, Characterization, and Biological Studies of Some Schiff Base Complexes. Russ. J. Coord. Chem. 2007; 33: 755-760.
10. Chohan ZH, Arif M, Akhtar MA, Supuran CT. Metal-Based Antibacterial and Antifungal Agents: Synthesis, Characterization, and In Vitro Biological Evaluation of Co(II), Cu(II), Ni(II), and Zn(II) Complexes With Amino Acid-Derived Compounds. Bioinorg. Chem. Appl. 2006; Article ID 83131: 1-13.
11. F. Yerly, F. A. Dunand, E. Toth, A. Figueirinha, Z. Kovacs, A. D. Sherry, Carlos F. G. C. Geraldes, A. E. Merbach, Spectroscopic Study of the Hydration Equilibria and Water Exchange Dynamics of Lanthanide(III) Complexes of 1,7-Bis(carboxymethyl)-1,4,7,10- tetraazacyclododecane (DO2A) Eur. J. Inorg. Chem. 2000; 1001-1006.

12. Yao M, Li Y, Hossu M, Joly AG, Liu Z, Liu Z, Chen W. Luminescence of Lanthanide Dimethyl Sulfoxide Compound Solutions. J. Phys. Chem. B. 2011; 115: 9352-9359.
13. Azab HA, Anwar ZM, Ahmed RG. Pyrimidine and Purine Mononucleotides Recognition by Trivalent Lanthanide Complexes with N-Acetyl Amino Acids. J. Chem. Eng. Data. 2010; 55: 459-475.
14. Zhang DW, Yang YJ, Ying SM, Liu YQ. Synthesis Neutral Rare Earth Complexes ofDiethylenetriamine-N, N''-bis(acetyl-o-hydroxybenzoyl hydrazide) -N, N', N-triacetic Acid as Potential Contrast Enhancement Agents for Magnetic Resonance Imaging. Synth. Reac. Inorg. Met-Org. Nano-Met. Chem. 2013; 43: 217-220.
15. Wang Q, Yang ZY, Qi GF, Qin DD. Crystal structures, DNA-binding studies and antioxidant activities of the Ln(III) complexes with 7-methoxychromone- 3-carbaldehyde-isonicotinoyl hydrazone. Biometals. 2010; 23: 1179-1189.
16. Kostova I, Stefanov T. Synthesis, characterization and cytotoxic/cytostatic activity of La(III) and Dy(III) complexes. J. Trace Elem. Med. Biol. 2010; 24: 7-13.
17. Wang BD, Yang ZY, Wang Q, Caib TK, Crewdson P. Synthesis, characterization, cytotoxic activities, and DNA-binding properties of the La(III) complex with Naringenin Schiff-base. Bioorg. Med. Chem. 2006; 14: 1880–1888.
18. Hussain A, Somyajit K, Banik B, Banerjee S, Nagaraju G, Chakravarty AR, Enhancing the photocytotoxic potential of curcumin on terpyridyl lanthanide(III) complex formation . Dalton Trans. 2013; 42: 182-195.
19. Durgo K, Halec I, Šola I, Franekić J. Cytotoxic and Genotoxic Effects of the Quercetin/Lanthanum Complex on Human Cervical Carcinoma cells in vitro. Arh. Hig. Rada. Toksikol. 2011; 62: 221-227.
20. Marinic´ M, Piantanida I, Rusak G, Z˘inic M. Interactions of quercetin and its lanthane complex with doublestranded DNA/RNA and single stranded RNA: Spectrophotometric sensing of poly G. J. Inorg. Biochem. 2006; 100: 288-298.
21. Mohanan K, Aswathy R, Nitha LP, Mathews NE, Sindhu Kumari B. Synthesis, spectroscopic characterization, DNA cleavage and antibacterial studies of a novel tridentate Schiff base and some lanthanide(III) complexes. J. Rare Earths. 2014; 32: 379-388.
22. Ansari AA, Sharma RK. Synthesis and Characterization of a Biologically Active Lanthanum(III)–Catechin Complex and DNA Binding Spectroscopic Studies. Spect. Lett. 2009; 42: 178-185.
23. Heffeter P, Popovic-Bijelic A, Saiko P, Dornetshuber R, Jungwirth U, Voevodskaya N, Biglino D, Jakupec MA, Elbling L, Micksche M, Szekeres T, Keppler BK, Gräslund A, Berger W, Ribonucleotide Reductase as One Important Target of [Tris(1,10-phenanthroline)lanthanum(III)] Trithiocyanate (KP772). Curr. Canc. Drug Targets. 2009; 9: 1-13.
24. Wang F, Huang W, Zhang Y, Wang M, Sun L, Tang B, Wang W. Determination of Protein by Fluorescence Enhancement of Curcumin in Lanthanum-Curcumin-Sodium Dodecyl Benzene Sulfonate-Protein System J. Fluoresc. 2011; 21: 25-34.
25. Refat MS, Al-Azab FM, Hussein MA, Al-Maydama, Amin RR, Yasmin Jamil MS, Synthesis and in vitro microbial evaluation of La(III), Ce(III), Sm(III) and Y(III) metal complexes of vitamin B6 drug. Spectrochim. Acta Part A. 2014; 127: 196-215.
26. Refat MS, Hussein MA, Al-Maydama, Al-Azab FM, Amin RR, Yasmin Jamil MS, Synthesis, thermal and spectroscopic behaviors of metal-drug complexes: La(III), Ce(III), Sm(III) and Y(III) amoxicillin trihydrate antibiotic drug complexes. Spectrochim Acta Part A. 2014; 128: 427-446.
27. Köse M, Ceyhan G, Atc E, McKee V, Tümer M, Synthesis, structural characterization and photoluminescence properties of a novel La(III) complex. J. Mol. Struc. 2015; 1088: 129-137.
28. Nadia EA, El-Gamel, Thermal studies, structural characterization, and antimicrobial evaluation of coordinated metal complexes containing salen moiety. Monatsh Chem. 2013; 144: 1627-1634.
29. Siddappa K, Sunilkumar BM, Manikprabhu D. La(III) complex involving the O,N-donor environment of quinazoline-4(3H)-one Schiff's base and their antimicrobial attributes against methicillin-resistant Staphylococcus aureus (MRSA). Spectrochim. Acta Part A. 2014; 130: 634-638.
30. Avaji PG, Badami PS, Patil SA, Synthesis, spectral, thermal, solid state d.c. electrical conductivity and biological studies of lanthanum(III) and thorium(IV) complexes with thiocarbohydrazone. Trans. Met. Chem. 2007; 32: 379-386.
31. Wang BD, Yang ZY, P. Crewdson, Wang DQ, Synthesis, crystal structure and DNA-binding studies of the Ln(III) complex with 6-hydroxychromone-3-carbaldehyde benzoyl hydrazone. J. Inorg Biochem. 2007; 10: 1492-1504.
32. S. Kobayashi, S. Kanai, Superoxide Scavenging Effects of Some Novel Bis-Ligands and Their Solvated Metal Complexes Prepared by the Reaction of Ligands with Aluminum, Copper and Lanthanum Ions. Molecules. 2013; 18: 6128-6141.
33. Perrin DD, Armarego WLF, Perrin DR, Purification of Laboratory Chemicals, Pergamon Press, Oxford, UK, 1980.
34. Schauer CL, Matwey E, Fowler FW, Lauher JW. Silver Coordination and Hydrogen Bonds: A Study of Competing Forces. Cryst. Eng. 1998; 1: 213-223.
35. Liu B, Wang HM, Yan SP, Liao DZ, Jiang ZH, Huang XY, Wang GL. Crystal structure of the addition compound of *N,N'*-bi(2-pyridylmethyl)-oxamide and complex of manganese with 1,10-phenanthroline. J. Chem. Cryst. 1999; 29: 623-627.
36. Ouyang Y, Liu B, Wang QL, Liao DZ, Jiang ZH, Yan SP, Three new copper(II)–nickel(II) heterodinuclear complexes with the N,N'-bis(2-pyridyl-ethyl)oxamide dianion. Syntheses, spectra, and magnetic properties. Trans. Met. Chem. 2005; 30: 460-463.
37. Marmur J. A procedure for the isolation of deoxyribonucleic acid from micro-organisms. J. Mol. Biol. 1961; 3: 208-218.
38. McGhee JD, von Hippel PH. Theoretical aspects of DNA protein interactions: cooperative and noncooperative binding of large ligands to a one-dimensional heterogeneous lattice. J. Mol. Biol. 1974; 86: 469-489.
39. LePecq JB, Paoletti C. A fluorescent complex between Ethidium bromide and nucleic acids. Physical-chemical characterization. J. Mol. Biol. 1967; 27: 87-106.
40. Kannan D, Arumugam MN, Synthesis, Characterisation, DNA-Binding Studies and antimicrobial activity of Copper (II) Complex with 1,10 Phenanthroline, L-Tyrosine and Thiosemicarbazide as Ligands. Elixir. Appl. Chem. 2014; 74: 27007-27104.
41. Chetana PR, Srinatha BS, Somashekar MN, Policegoudra RS. Synthesis, spectroscopic characterisation, thermal analysis, DNA interaction and antibacterial activity of copper(I) complexes with *N,N'*- disubstituted thiourea. J. Mol. Struc. 2016; 1106: 352-365.
42. Bernadou J, Pratviel G, Bennis F, Girardet M, Meunier B. Potassium Monopersulfate and a Water-Soluble Manganese Porphyrin Complex, [Mn(TMPyP)](OAC)$_5$, as an Efficient Reagent for the Oxidative Cleavage of DNA. Biochemistry. 1989; 28: 7268-7275.
43. Chetana PR, Rao R, Saha S, Policegoudra RS, Vijayan P, Aradhya MS. Oxidative DNA cleavage, cytotoxicity and antimicrobial studies of L-ornithine copper (II) complexes. Polyhedron. 2012; 48: 43-50.
44. Zaidan MRS, Rain AN, Badrul AR, Adlin A, Norazah A, Zakiah I. *In vitro* screening of five local medicinal plants for antibacterial activity using disc diffusion method. Trop. Biomed. 2005; 22: 165-170.

45. Bauer AW, Kirby WMM, Serris JC, Turck M. Antibiotic susceptibility testing by a standardized single disc method. Am. J. Clin. Path. 1966; 45: 493-496.
46. Chetana PR, Somashekar MN, Srinatha BS, Policegoudra RS, Aradhya SM, Rao R. Synthesis, Crystal Structure, Antioxidant, Antimicrobial, and Mutagenic Activities and DNA Interaction Studies of Ni(II) Schiff Base 4-Methoxy-3-benzyloxybenzaldehyde Thiosemicarbazide complexes. ISRN Inorg. Chem. 2013; Article ID 250791: 11 pages.
47. Brand-Williams W, Cuvelier ME, Berset C. Use of a free radical method to evaluate antioxidant activity. Lebensm.-Wiss. u.-Technol. 1995; 28: 25-30.
48. Wang T, Jónsdóttir R, Ólafsdóttir G. Total phenolic compounds, radical scavenging and metal chelation of extracts from Icelandic seaweeds. Food Chem. 2009; 116: 240-248.
49. Policegoudra RS, Abiraj K, Gowda DC, Aradhya SM. Isolation and characterization of antioxidant and antibacterial compound from mango ginger (*Curcuma amada* Roxb.) rhizome. J. Chrom. B. 2007; 852: 40-48.
50. Hegde SM, Kumar MN, Kavya K, Kumar KMK, Nagesh R, Patil RH, Babu RL, Ramesh GT, S.C. Sharma, Interplay of nuclear receptors (ER, PR, and GR) and their steroid hormones in MCF-7 cells. Mol. Cell. Biochem. 2016; 422: 109-120.
51. Patil RH, Babu RL, Kumar MN, Kumar KMK, Hegde SM, Ramesh GT, Sharma SC. Apigenin inhibits PMA-induced expression of pro-inflammatory cytokines and AP-1 factors in A549 cells. Mol. Cell. Biochem. 2015; 403: 95-106.
52. Taidakov IV, Strelenko YA, Borisov RS, Temerdashev AZ, Datskevich NP, Vitukhnovskii AG. Yttrium(III) and Lanthanum(III) Tris(1,3-Bis(1,3-Dimethyl-1*H* Pyrazol-4-yl)propane-1,3-Dionato)(1,10-Phenanthroline): Synthesis and Study by Mass Spectrometry, X-ray Diffraction Analysis, and ^{89}Y and ^{139}La NMR Spectroscopy. Russian J. Coord. Chem. 2015; 41: 230-239.
53. Gumus G, Gurol I, Yuksel F, Gurek AG, Ahsen V. Alkyl-substituted oxamide oximes and their metal complexes. Polyhedron 2012; 33: 45-51.
54. Li XJ, Zheng K, Li YT, Yan CW, Wu ZY, Xuan SY. Synthesis and structure of a 1-D copper(II) coordination polymer bridged both by oxamido and carboxylate: in vitro anticancer activity and reactivity toward DNA and protein BSA. J. Coord. Chem. 2015; 68: 928-948.
55. Wang Y, Yang ZY, Wang Q, Cai QK, Yu KB. Crystal structure, antitumor activities and DNA-binding properties of the La(III) complex with Phthalazin-1(2H)-one prepared by a novel route. J. Organomet. Chem. 2005; 690: 4557-4563.
56. Perumal G, Dharmasivam M, Prabhu D, Arulvasu C, Rahiman AK. Mixed-ligand copper(II) phenolate complexes: Synthesis, spectral characterization, phosphate-hydrolysis, antioxidant, DNA interaction and cytotoxic studies J. Mol. Struc. 2015; 1080: 88-98.
57. Sigman DS. Chemical Nucleases. Acc. Chem. Res. 1986; 19: 180-186.
58. Badwaik VB, Aswar AS. Synthesis, Characterization, and Biological Studiesof Some Schiff Base Complexes. Russ. J. Coord. Chem. 2007; 33: 755-760.
59. Binil PS, Anoop MR, Jisha KR, Suma S, MR Sudarsanakumar. Synthesis, spectral characterization, thermal and biological studies of lanthanide(III) complexes of oxyphenbutazone. J. Rare Earths. 2014; 32: 43-51.
60. Rehman M, Imran M, Arif M. Synthesis, Characterization and in vitro Antimicrobial studies of Schiff-bases derived from Acetyl acetone and Amino acids and their Oxovanadium(IV) complexes. Am. J. Appl. Chem. 2013; 1: 59-66.
61. Abbs TF, Reji F, PearlAJ, Rosy BA. Synthesis, characterization, cytotoxicity, DNA cleavage and antimicrobial activity of homodinuclear lanthanide complexes of phenylthioacetic acid. J. Rare Earths. 2013; 3: 1009-1016.

HOW TO CITE THIS ARTICLE: Chetana PR, Bhat VV, Dhale MA. Hetero-Binuclear Complexes of Lanthanum (III) Using Bridging *N,N'*-Bis(2-Pyridylmethyl)Oxamide and Terminal 1,10-Phenanthroline: Synthesis, Characterization and Biological Evaluation. Int. J. Pharm. Sci. Drug Res. 2018; 10(6): 460-473. **DOI: 10.25004/IJPSDR.2018.100606**